CATEGORIZED CRATER COUNTS ON MARTIAN LOBATE DEBRIS APRONS. Daniel C. Berman, David A. Crown, and Emily C.S. Joseph, Planetary Science Institute, 1700 E. Ft. Lowell Rd., Suite 106, Tucson, AZ 85719; bermandc@psi.edu.

Introduction: The Martian mid-latitudes are of high scientific interest as they are regions where the effects of ice on the surface geology are prominent [e.g., 1-5]. Mid-latitude glacial activity has been interpretated to have occurred throughout the Amazonian Period. Some studies have proposed large-scale glaciation in the Late Amazonian [e.g., 6-8]. Our new results indicate a long history of glacial activity, beginning in the Early Amazonian with the formation of lobate debris aprons, extending to ice-rich mantling in the Late Amazonian. We have developed a new approach for analyzing crater size-frequency distributions designed to interpret formation and modification ages from complex geologic surfaces, such as those of ice-rich debris aprons. In conjunction with textural analyses of apron surfaces, we have counted and characterized the morphologies of small craters on apron surfaces in order to constrain their geologic history.

Morphologic Characteristics of Small Impact Craters on Apron Surfaces: We have examined impact craters on apron surfaces to assess typical sequences of crater degradation that help to interpret crater-size frequency distributions (SFD). Craters exhibit fresh, degraded, and filled morphologies. For accurate age interpretations, we need to understand degradational morphologies and to discriminate populations that provide age constraints on deposits that mantle apron surfaces from those that represent the formation/emplacement of the apron mass.

Crater Count Methodology: Crater SFD statistics have been compiled using established methodologies [9-12]; all impact craters (primaries and isolated secondaries) on a given surface in a specific diameter range are counted while avoiding areas of obvious secondary chains or clusters. These data are then plotted on the isochrons defined by [10-12] to assess relative age (Martian time-stratigraphic age) and determine a diameter range or ranges that "fit" the isochrons. This fit range is then used to derive absolute ages using Craterstats2 software. Deviations from isochron shape over specific crater size ranges, along with categorization of crater type provide further information on erosional and depositional processes affecting the surfaces of interest.

Potentially ice-rich surfaces can be geologically complex given uncertainties in ice content and distribution, and mantling and degradational history. In mid-latitude zones, surfaces may have undergone multiple cycles of mantling. We assume fresh (bowl-shaped) craters superpose even the youngest of these and that filled craters are filled with mantling deposits and thus indicate a formation or stabilization age of the landform/surface that has been mantled. Layered mantling deposits on the floors of craters, as well as degradational textures resembling mantle materials on surrounding surfaces support this interpretation. Degraded craters may have formed before the most recent mantling episode, but have not accumulated much fill.

Study Areas: We have conducted crater count analyses using CTX images on lobate debris aprons in the Deuteronilus Mensae region along the dichotomy boundary [cf., 13] and in the region east of Hellas Basin. In eastern Hellas, craters have been counted and categorized on 17 separate aprons, with a total area of 14,024 km^2. In Deuteronilus Mensae, we have counted craters on two large complexes of aprons (northern and central) with a total area of 13,442 km^2 (5,113 km^2 of which have been categorized).

East Hellas Debris Apron SFD: The distribution of all craters superposed on all 19 debris aprons in eastern Hellas shows an age of ~400 My. Individual aprons show a range of ages, from 10s of Ma to several Ga. For *all craters* on debris apron 12 in eastern Hellas, for example (Fig. 1), a segment follows the isochrons (~250 m – 707 m), indicating a formation age of ~400 Ma during the Middle Amazonian. The distribution of *filled craters* mimics that for all (and degraded) craters but the depletion of small crater sizes (relative to the isochrons) is greater, consistent with degradation due to erosion or sublimation, giving an apron stabilization age of ~300 Ma. *Fresh craters* show a maximum mantling age of ~2 Ma (based on the largest bins with more than one crater), consistent with ice deposition during a period of high obliquity.

Examination of age constraints for individual aprons provides new insights into the potential age range for the regional apron population as well as local and regional effects that may have caused differences in degradation of apron surfaces across eastern Hellas. The shapes of the SFDs and the multiple ages apparent for individual aprons are consistent with the complex formation and modification histories of debris apron surfaces indicated by the characterization of surface textures and morphology. Individual aprons show different ages within the Hellas population, and sometimes multiple ages are evident for the same apron, over a range from 10s of Ma to ~1000 Ma.

Deuteronilus Mensae Debris Apron SFD: The distribution of *all craters* superposed on the northern debris apron complex in the study area (complex A, Fig. 2) shows one segment that follows the isochrons (~500 m - 1 km), indicating a formation age of ~1.1 Ga during the Early Amazonian Epoch (error range spanning Early to Middle Amazonian). As in eastern Hellas, the distribution of *filled craters* mimics that for *all craters*, matching the isochron slope from the 500 m to 1 km bins, but the depletion of small crater sizes (relative to the isochrons) is greater, consistent with mantled debris apron surfaces and show an age since stabilization of the apron of ~900 Ma ago. The distribution of *fresh craters* does not match the isochrons, but shows a maximum mantling age of ~3 Ga, consistent with the several-My age estimates of obliquity-driven mid-latitude mantling deposits.

Discussion: The various potential mantling and resurfacing ages estimated from debris aprons can be attributed to a combination of highly mobile surface materials, the presence of ice and the degradational effects of loss of ice, and a complex history of erosion and mantling [3]. Craters of various morphologic types are observed on eastern Hellas and Deuteronilus Mensae debris aprons and analyses of their population statistics by morphology reveal different categories of ages. The filled craters, which may reveal minimum apron formation ages at large diameters (>~500 m), generally show the oldest ages in the range of several 100s of Ma to ~1 Ga (Fig. 3). At smaller diameters (~100 m to 500 m), resurfacing ages between ~10 Ma and several 100s of Ma may be revealed as the distribution fits younger isochrons for all or filled craters; these intermediate ages suggest a complex history of degradation and mantling prior to stabilization of a surface that accumulates craters according to the production function. Small fresh craters (generally smaller than ~100 m in diameter) reveal the youngest ages, typically less than ~10 Ma, likely the ages of recent mantling episodes.

References: [1] Berman D.C. et al. (2005) *Icarus 178*, 465-486. [2] Berman D.C. et al. (2009) *Icarus 200*, 77-95. [3] Christensen P.R. (2003) *Nature 422*, 45-48. [4] Head J.W. et al. (2003) *Nature 426*, 797-802. [5] Mustard, J.F., et al. (2001) *Nature 412*, 411-414. [6] Head J.W. et al. (2006) *EPSL 241*, 663-671. [7] Head J.W. et al. (2005) *Nature 434*, 346-351. [8] Crown D.A. et al. (2005) *JGR 110*. [9] Berman D.C, and Hartmann W.K. (2002) *Icarus, 159*, 1-17. [10] Hartmann W.K. (2005) *Icarus, 174*, 294-320. [11] Hartmann W.K. (2007) *7th Intl. Conf. on Mars, abstract 3318*. [12] Hartmann W.K. (2007) *Icarus, 189*, 274-278. [13] Chuang F.C. and Crown D.A. (2009) USGS Map 3079.

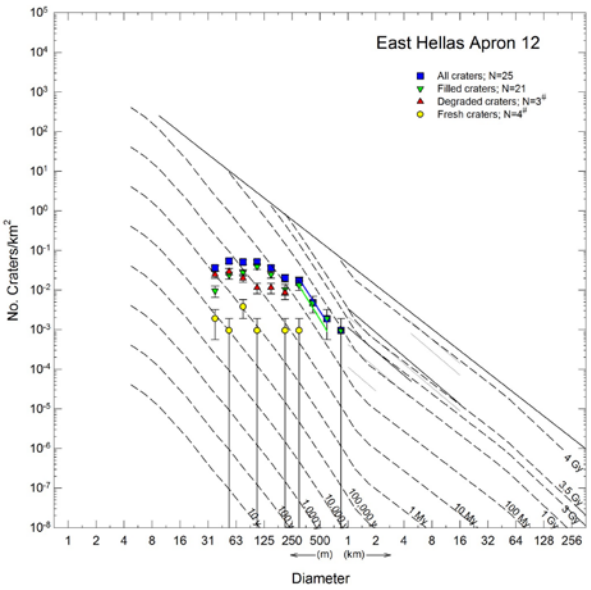

Figure 1. Crater SFD for lobate debris apron 12 in eastern Hellas.

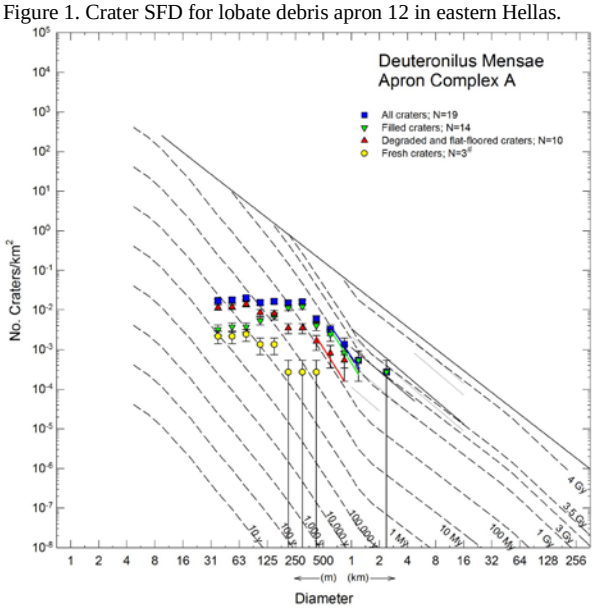

Figure 2. Crater SFD for debris apron complex A in DM.

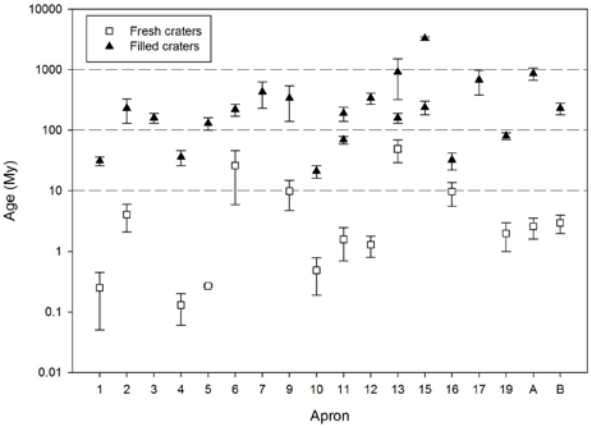

Figure 3. Plot of ages (or maximum ages) for filled and fresh craters for each apron.